*Transactions of the Korean Nuclear Society Spring Meeting*
*Jeju, Korea, May 22-23, 2025*

# Modeling of Hydrogen and Carbon Monoxide Recombination by a Passive Autocatalytic Recombiner for Nuclear Reactor Containment Safety

Jongtae Kim [a*]
[a] *KAERI, Daeduk-daero 989-111, Daejeon, Korea*
[*] *Corresponding author: ex-kjt@kaeri.re.kr*

***Keywords :** hydrogen, carbon monoxide, passive autocatalytic recombiner, nuclear reactor, containment

## 1. Introduction

In current power plants with pressurized water reactors, hydrogen mitigation system (HMS) using passive auto-catalytic recombiners (PAR) is installed to control a hydrogen concentration during design-based or severe accidents. It is recently understood that PAR can recombine carbon monoxide which can be produced by molten corium concrete interaction (MCCI).

Carbon monoxide generated by an MCCI accidental event is also belonging to a combustible gas with hydrogen during a severe accident of a pressurized water reactor. So, it must be considered as one of the flammable gas explosion threats within the reactor containment, along with hydrogen.

Currently, research on the carbon monoxide recombination characteristics of PAR is being conducted in many countries, but PAR vendors except Framatome still do not provide a correlation equation for carbon monoxide removal rates.

Kim et al. [1] introduced a generic PAR model based on gas species diffusion mass fluxes. In this study, the diffusion-controlled PAR model has been extended to consider hydrogen and carbon monoxide recombination by PAR.

## 2. Modeling

As a PAR catalytic reaction rate, a correlation equation based on hydrogen removal rate data obtained from PAR performance tests is generally used as shown in Eq. (1),

$$R = correlation(p,\ T,\ x_{h2},\ x_{o2},\ x_{h2o}) \qquad (1)$$

Currently, most PAR correlations, except Framatome PAR, do not reflect the removal rate for carbon monoxide.

Reinecke [2] stated that the rate of hydrogen removal by PAR depends on the rate of hydrogen diffusion because the diffusion rate is slower than the rate of surface catalysis.

A PAR model based on the hydrogen mass diffusion rate is so general that it can, in principle, be applied to carbon monoxide recombination by the PAR. The mass diffusion coefficient of each gas species on a catalytic surface can be obtained by a Sherwood number correlation such as for a flat plate.

The oxidation reaction of hydrogen and carbon monoxide by PAR catalyst goes through many chemical reaction steps. Here, it is assumed that the diffusion rate of gaseous components dominates the recombination rate of PAR because the diffusion rate is slower than that of other chemical reaction steps. Eqs. (2) and (3) represent the single-step chemical reaction of hydrogen and carbon monoxide and the reaction heat per unit mass, respectively.

$$H_2 + \frac{1}{2}O_2 \Rightarrow\ H_2O + 121\ MJ/kg \qquad (2)$$

$$CO + \frac{1}{2}O_2 \Rightarrow\ CO_2 + 10\ MJ/kg \qquad (3)$$

The chemical reaction rates of Eqs. (1) and (2) can be expressed by the diffusion rates of each gaseous component. Eqs. (3), (4), and (5) are the mass fluxes supplied to the catalyst surface by the diffusion rates of hydrogen, carbon monoxide, and oxygen.

$$\phi_{H_2} = \rho h_{m,H_2} Y_{H_2} \qquad (4)$$

$$\phi_{CO} = \rho h_{m,\mathrm{CO}} Y_{CO} \qquad (5)$$

$$\phi_{O_2} = \rho h_{m,O_2} Y_{O_2} \qquad (6)$$

The diffusion coefficient $h_m$ of the gas component is obtained using the Sherwood number correlation as follows. The Sherwood number correlation is expressed as a function of the Gr number in the case of natural convection and as a function of the Re number in the case of forced convection, depending on the flow characteristics. Here, since three-dimensional modeling is performed for the catalyst reaction region and the housing region, the Sherwood number correlation based on the Reynolds (Re) and Schmidt (Sc) numbers, as in Eq. (9), is used.

$$Re_L = \rho_g U_g L_{par}/\mu_g \qquad (7)$$

$$Sc = \nu_g/D \qquad (8)$$

$$Sh = \frac{h_m L_{par}}{D} = \begin{cases} 0.664 Re_L^{1/2} Sc_{H_2}^{1/3},\ Re_L < 5 \times 10^5 \\ 0.037 Re_L^{4/5} Sc_{H_2}^{1/3},\ Re_L > 5 \times 10^5 \end{cases} \qquad (9)$$

Eqs. (4) and (5) can be applied when sufficient oxygen is supplied for the oxidation reaction of hydrogen and carbon monoxide, but in the general containment environment during an accident, oxygen continuously decreases, resulting in an oxygen-deficient environment. When the oxygen concentration of the gas flowing into the PAR is low, the PAR recombination rate is affected by the oxygen concentration. Through several experiments on oxygen-lean conditions through the THAI and THEMIS projects, it was confirmed that the recombination efficiency decreases when oxygen is lean, and the oxygen surplus ratio, which means the concentration of oxygen to the concentration of combustible gas, is defined as follows. Eq. (10) represents oxygen surplus ratio for hydrogen recombination and Eq. (11) is for hydrogen and carbon monoxide recombination.

$$\Phi = 2x_{O_2}/x_{H_2} \tag{10}$$

$$\Phi = 2x_{O_2}/(x_{H_2} + x_{CO}) \tag{11}$$

Framatome PAR defines the recombination efficiency of the PAR according to the oxygen surplus ratio $\Phi$ as shown in Eq. (12). In this study, Eq. (13) is used so that the recombination efficiency linearly decreases with the oxygen surplus ratio.

$$\eta = \begin{cases} 1 & \Phi \geq 2 \\ 0.6 & \Phi < 2 \end{cases} \tag{12}$$

$$\eta = max[0.6, min(1, 0.5\phi)] \tag{13}$$

Fig. 1 is a graphical comparison of the recombination efficiency Eqs. (12) and (13) according to the oxygen surplus ratio $\Phi$. These equations set the lower limit of the oxygen surplus ratio $\Phi_{lim}$ to 2, but the THAI experimental results confirmed that it can vary depending on the characteristics of the PAR product type.

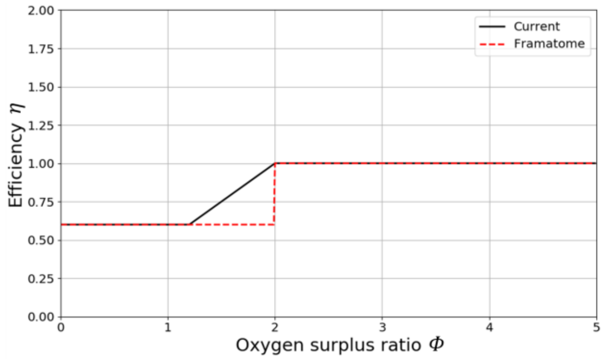

Fig. 1. PAR recombination efficiency depending on oxygen surplus ration.

In an atmosphere where only hydrogen is present as a combustible gas, the recombination rate of hydrogen is determined as follows by the stoichiometric ratio of Eq. (2).

$$\dot{R} = \eta \cdot min\left(\dot{m}_{H_2},\ \frac{1}{8}\dot{m}_{O_2}\right) \tag{14}$$

Here, the hydrogen mass removal rate $\dot{m}_{H_2}$ is the product of the diffusion mass flux and the catalyst surface area as such $\dot{m}_{H_2} = \phi_{H_2} A_{cat}$. When oxygen is sufficiently supplied to the catalyst of a PAR, the catalytic reaction of stoichiometric ratio can occur as in Eqs. (2) and (3). The mass removal rate of oxygen required at this time is as follows.

$$\begin{aligned} \dot{m}_{O_2,req} &= \dot{m}_{O_2 byH_2} + \dot{m}_{O_2 byCO} \\ &= \frac{W_{O_2}}{2W_{H_2}}\dot{m}_{H_2} + \frac{W_{O_2}}{2W_{CO}}\dot{m}_{CO} \end{aligned} \tag{15}$$

, where $W_i$ is a molecular weight of a species i with the dimension of [kg/kmol].

The amount of oxygen participating in the catalytic reaction is also governed by the diffusion rate in Eq. (6), just like hydrogen or carbon monoxide.

In the case that a diffusion mass flow of oxygen is greater than the required oxygen mass flow ( $\dot{m}_{O_2} \geq \dot{m}_{O_2,req}$), the recombination rate of hydrogen and carbon monoxide is not limited by oxygen as follows with $\eta$ depending on $\Phi$.

$$\dot{R}_{CO} = \eta \cdot \dot{m}_{CO} \tag{16}$$

$$\dot{R}_{H_2} = \eta \cdot \dot{m}_{H_2} \tag{17}$$

Conversely, when oxygen is starved and $\dot{m}_{O_2} < \dot{m}_{O_2,tot}$, it is affected by the oxygen diffusion rate. In this case, it can be assumed that hydrogen and carbon monoxide share oxygen in the same ratio as the stoichiometric ratio.

$$\gamma = \dot{m}_{O_2 byCO}/\dot{m}_{O_2,req} \tag{18}$$

$$\dot{R}_{CO} = \eta \cdot \gamma \cdot \dot{m}_{O_2}(2W_{CO}/W_{O_2}) \tag{19}$$

$$\dot{R}_{H_2} = \eta \cdot (1-\gamma) \cdot \dot{m}_{O_2}(2W_{H_2}/W_{O_2}) \tag{20}$$

Meanwhile, considering that the reaction rate between carbon monoxide and oxygen is slower than that between hydrogen and oxygen, a model can be assumed in which carbon monoxide is oxidized first, and then hydrogen is oxidized with the remaining oxygen.

$$\dot{R}_{CO} = \eta \cdot \dot{m}_{CO} \tag{21}$$

$$\dot{R}_{H_2} = \eta \cdot \left(\dot{m}_{O_2} - \dot{m}_{CO}\frac{W_{O_2}}{2W_{CO}}\right)\frac{2W_{H_2}}{W_{O_2}} \tag{22}$$

The recombination rates of hydrogen and carbon monoxide are included in the source terms of the respective mass conservation equations, as in Eqs. (23) and (24). The consumption and production rates of oxygen, water vapor, and carbon dioxide are as in Eqs. (25 ~ 27).

$$S_{CO} = -\dot{R}_{CO} \tag{23}$$

$$S_{H_2} = -\dot{R}_{H_2} \tag{24}$$

$$S_{O_2} = -\frac{W_{O_2}}{2W_{CO}}\dot{R}_{CO} - \frac{W_{O_2}}{2W_{H_2}}\dot{R}_{H_2} \tag{25}$$

$$S_{H_2O} = \frac{w_{H_2O}}{w_{H_2}} \dot{R}_{H_2} \qquad (26)$$

$$S_{CO_2} = \frac{w_{CO_2}}{w_{CO}} \dot{R}_{CO} \qquad (27)$$

## 3. Validation Results

Freitag et al. [3] performed hydrogen and carbon monoxide recombination experiments HR-51 and HR-53 using the THAI test facility. The HR-51 test was an experiment in which carbon monoxide and hydrogen were injected under initial dry air conditions, and the HR-53 experiment was performed under a wet air atmosphere.

Table 1 shows the initial temperature, pressure, and water vapor concentration of the two experiments.

Table 1. Test conditions for HR-51 and HR-53 tests

| Test name | Pressure [bar] | Temperature [oC] | Steam [vol%] |
|---|---|---|---|
| HR-51 | 1.5 | 25 | 0 |
| HR-53 | 3.0 | 117 | 60 |

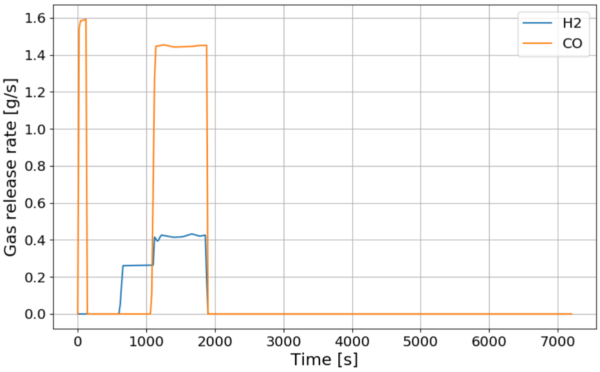

Fig. 2. Injection mass flow of H2 and CO in test HR-51.

Fig. 2 shows the hydrogen and carbon monoxide injection mass flow rates over time for the HR-51 test.

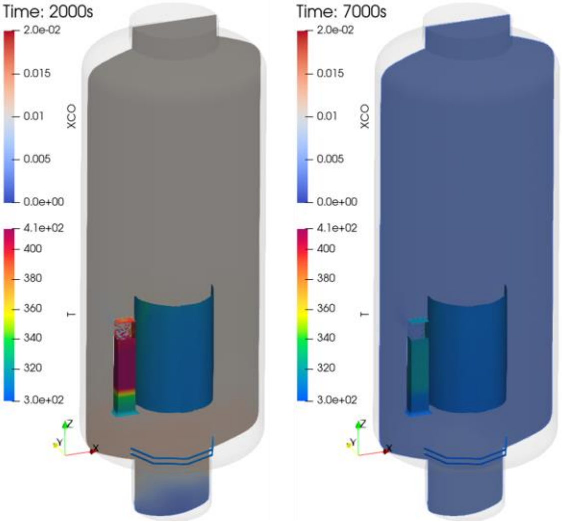

Fig. 3. Distributions of CO concentration and temperature of PAR housing at 2000s and 7000s for HR-51 test.

Fig. 3 shows the carbon monoxide concentration distribution inside the THAI pressure vessel and the surface temperature of the PAR housing at 2,000 and 7,000 seconds based on the calculation results of HR-51. At 2,000 seconds after the injection of carbon monoxide, the carbon monoxide concentration is distributed in the range of about 1 ~ 2% and is higher in the region below the PAR. In addition, it can be seen that the temperature of the housing surface rises significantly due to the catalytic reaction of the PAR. After 7,000 seconds from the start of the experiment, the carbon monoxide concentration appears to be distributed almost uniformly close to 0.

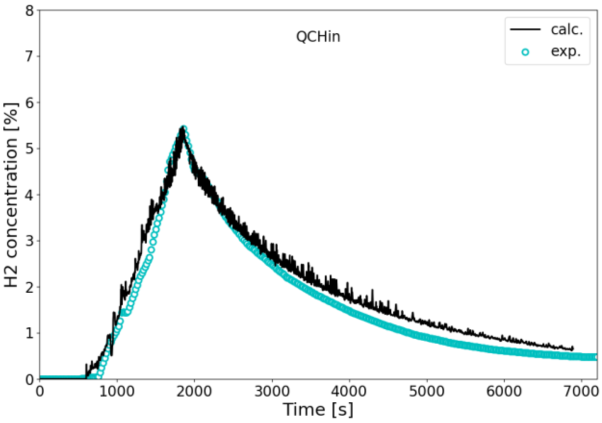

Fig. 4. PAR inlet $H_2$ concentration over time for HR-51 test

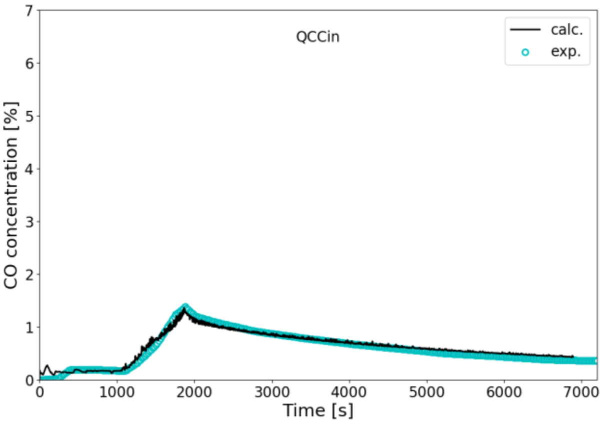

Fig. 5. PAR inlet CO concentration over time for HR-51 test

Figs. 4 and 5 compare the time-dependent concentration changes of hydrogen and carbon monoxide flowing into the PAR inlet with the experimental results. It can be seen that the calculated results are generally in good agreement with the experimental results.

Fig. 6 shows the removal rates of hydrogen and carbon monoxide by PAR in the HR-51 test. The calculated recombination rate of hydrogen by PAR is very consistent with the experimental results, but the recombination rate of carbon monoxide has some period when it differs from the experimental data. In the current study Eqs. (21) and (22) were used. It is thought that the other method by Eqs. (19) and (20) need to be considered.

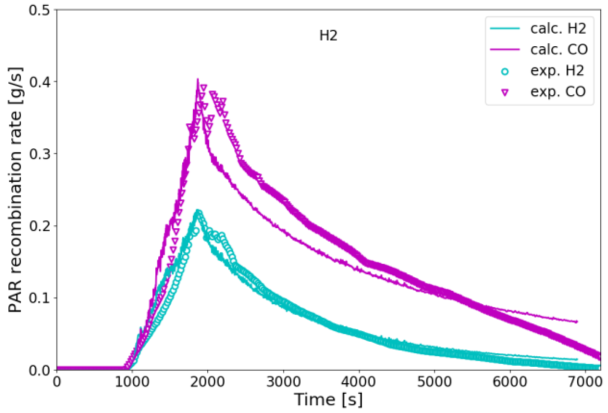

Fig. 6. Comparison of hydrogen and carbon monoxide removal rates by the PAR in the HR-51 test.

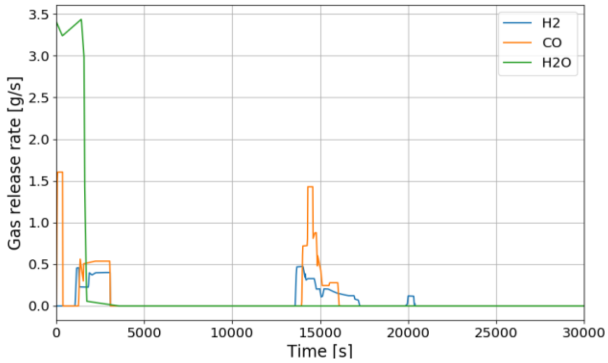

Fig. 7. Injection mass flow of H2, CO and H2O in test HR-53.

Fig. 7 shows the injection mass flow rates of hydrogen, carbon monoxide, and water vapor over time in the HR-53 test. The HR-53 test is an experiment that injects hydrogen and carbon monoxide into a water vapor atmosphere, simulating an oxygen-deficient condition.

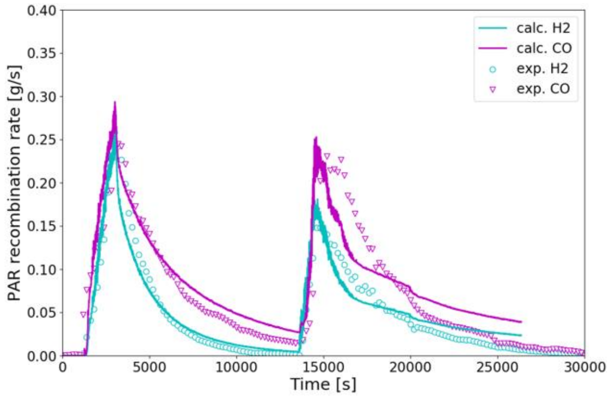

Fig. 8. Comparison of hydrogen and carbon monoxide removal rates by the PAR in the HR-53 test.

Fig. 8 shows the removal rates of hydrogen and carbon monoxide by PAR in the HR-53 test. It shows that hydrogen and carbon monoxide recombination rates increase during injected and the recombination rates slowly decrease during a period of no injection of hydrogen and carbon monoxide. It depicts that the recombination rate of the carbon monoxide has a discrepancy compared with the experimental data which will be re-considered in a future study.

## 4. Conclusions

In this study, the diffusion-controlled PAR model has been extended to consider hydrogen and carbon monoxide recombination. The gas species diffusion-based recombination model reasonably reproduces the experimental results.

It is thought that the diffusion-based recombination model is applicable to a safety analysis of a severe accident with MCCI.

## ACKNOWLEDGMENTS

This work was supported by the Korea Foundation of Nuclear Safety (KOFONS) (No. 2106007).

## REFERENCES

[1] J. Kim, et al., Establishment of a base system for 3D analysis of hydrogen distribution in a containment building, KINS Contract Report, 2022

[2] E.-A. Reinecke et al., "Simulation of the efficiency of hydrogen recombiners as safety devices". Int. J. of Hydrogen Energy, 38, 8117-8124, 2013.

[3] M. Freitag, B. von Laufenberg, M. Colombet, M. Klauck, "Measurements of the impact of carbon monoxide on the performance of passive autocatalytic recombiners at containment-typical conditions in the THAI facility", Annals of Nuclear Energy 141, 107356, 2020.